Immunity
Article

T Cell Allorecognition via Molecular Mimicry

Whitney A. Macdonald,[1] Zhenjun Chen,[2] Stephanie Gras,[1] Julia K. Archbold,[1] Fleur E. Tynan,[1] Craig S. Clements,[1] Mandvi Bharadwaj,[2] Lars Kjer-Nielsen,[2] Philippa M. Saunders,[2] Matthew C.J. Wilce,[1] Fran Crawford,[4] Brian Stadinsky,[4] David Jackson,[2] Andrew G. Brooks,[2] Anthony W. Purcell,[3] John W. Kappler,[4] Scott R. Burrows,[5] Jamie Rossjohn,[1,6,*] and James McCluskey[2,6,*]

[1]The Protein Crystallography Unit, Department of Biochemistry and Molecular Biology, Monash University, Clayton, Victoria 3800, Australia
[2]Department of Microbiology & Immunology
[3]Department of Biochemistry and Molecular Biology and Bio21 Molecular Science and Biotechnology Institute
University of Melbourne, Parkville, Victoria 3010, Australia
[4]Howard Hughes Medical Institute, Integrated Department of Immunology, National Jewish Health, 1400 Jackson Street, Denver, CO 80206, USA
[5]Cellular Immunology Laboratory, Queensland Institute of Medical Research and Australian Centre for Vaccine Development, Brisbane, 4029, Australia
[6]These authors contributed equally to this work
*Correspondence: jamie.rossjohn@med.monash.edu.au (J.R.), jamesm1@unimelb.edu.au (J.M.)
DOI 10.1016/j.immuni.2009.09.025

SUMMARY

T cells often alloreact with foreign human leukocyte antigens (HLA). Here we showed the LC13 T cell receptor (TCR), selected for recognition on self-HLA-B*0801 bound to a viral peptide, alloreacts with B44 allotypes (HLA-B*4402 and HLA-B*4405) bound to two different allopeptides. Despite extensive polymorphism between HLA-B*0801, HLA-B*4402, and HLA-B*4405 and the disparate sequences of the viral and allopeptides, the LC13 TCR engaged these peptide-HLA (pHLA) complexes identically, accommodating mimicry of the viral peptide by the allopeptide. The viral and allopeptides adopted similar conformations only after TCR ligation, revealing an induced-fit mechanism of molecular mimicry. The LC13 T cells did not alloreact against HLA-B*4403, and the single residue polymorphism between HLA-B*4402 and HLA-B*4403 affected the plasticity of the allopeptide, revealing that molecular mimicry was associated with TCR specificity. Accordingly, molecular mimicry that is HLA and peptide dependent is a mechanism for human T cell alloreactivity between disparate cognate and allogeneic pHLA complexes.

INTRODUCTION

Clonally distributed αβ T cell receptors (TCR) corecognize specific antigenic peptides bound to polymorphic human leukocyte antigens (HLA) of the major histocompatibility complex (MHC) (Davis et al., 1998; Rudolph et al., 2006). HLA polymorphism ensures that the HLA molecules from different haplotypes can bind a broad sample of self and microbial peptide antigens necessary to mediate adaptive immunity (Parham and Ohta, 1996). Developing T cells in the thymus are selected for weak recognition of one or more of the many self-peptide-HLA complexes (Bevan and Hünig, 1981; Hogquist et al., 1993) generating a large repertoire of T cells, each expressing individual TCRs (Fink and Bevan, 1995). Inherent structural plasticity of the TCR contributes to chance improvements in recognition of novel peptide-HLA complexes (pHLA) that are generated when self-peptides are replaced with foreign peptides during infection (Garcia et al., 1998, 1999; Rudolph et al., 2006). This recognition triggers effector immunity by responsive T cells.

Despite pHLA diversity and TCR plasticity, αβ-T cell responses remain exquisitely specific (Archbold et al., 2009) and are developmentally restricted to recognizing host (self) HLA (Jameson et al., 1995; Zinkernagel and Doherty, 1974), with the exception of minor subpopulations like NKT cells (Borg et al., 2007). This "genetic restriction" of MHC-directed T cell immunity means that T cells recognize only cognate antigen presented by one of the host HLA molecules in which they developed (also termed MHC restriction) (Zinkernagel and Doherty, 1974). This "law" of immunology is a defining paradigm of antigen-specific T cell immunity (Garboczi and Biddison, 1999).

Surprisingly, some T cells break the "law" of MHC restriction (Sherman and Chattopadhyay, 1993) by directly reacting with "foreign" HLA molecules from unrelated (allogeneic) individuals. HLA polymorphism involving just one amino acid, or up to 30 or more residues, can induce an immune response toward transplanted cells, the severity of which is variable. Thus, some HLA mismatches lead to worse transplant outcomes than others, so-called taboo mismatches (Doxiadis et al., 1996; Kawase et al., 2007). For instance, mismatching across closely related HLA allotypes such as HLA-B*4402 and HLA-B*4403 provokes vigorous T cell alloreactivity (Mifsud et al., 2008) associated with transplant rejection (Fleischhauer et al., 1990) and acute graft-versus-host disease (Keever et al., 1994) after haemopoietic stem cell transplantation, despite the broadly similar peptide repertoires of these allotypes (Macdonald et al., 2003). In contrast, highly divergent HLA mismatches may paradoxically have a better outcome in some transplant settings (Heemskerk et al., 2007). Regardless, T cell alloreactivity is responsible for much of the morbidity and mortality associated with tissue transplantation, including graft-versus-host disease (Afzali et al.,

2007), making this unexplained contradiction to the phenomenon of MHC restriction of great clinical importance.

The paradox of alloreactivity has remained a mystery for more than three decades (Archbold et al., 2008b; Dröge, 1979; Lechler and Lombardi, 1990), including the reasons for the high frequency of these T cells (Lindahl and Wilson, 1977) and whether the peptide or the HLA molecule is more important in driving T cell alloreactivity (Bevan, 1984; Matzinger and Bevan, 1977). The HLA-centric model of alloreactivity considers that T cells concentrate on the polymorphic HLA residues irrespective of the bound peptide. For instance, the alloreactive murine 2C TCR adopts two very different binding orientations when bound to its host selecting-pMHC ligand versus an allogeneic pMHC target ligand, focusing instead on a mixture of allogeneic MHC differences and new peptide contacts (Colf et al., 2007; Rossjohn and McCluskey, 2007). In contrast, the peptide-centric theory of allorecognition implies that the TCR exploits the similarities between the allogeneic and self-HLA molecule (''mimicry'') and recognizes the new set of endogenous peptides as foreign. Additionally, molecular mimicry is considered to underpin numerous T cell autoimmune disorders but has nevertheless been difficult to establish given the explicit requirement of the TCR to corecognize the antigens as well as the HLA molecules. Moreover, limited evidence so far suggests that T cell allorecognition is peptide centric (Archbold et al., 2008a; Colf et al., 2007; Reiser et al., 2000; Speir et al., 1998) and implicates polyspecificity as a mechanism leading to the high frequency of alloreactive T cells (Felix et al., 2007). However, it is still unclear whether dual recognition of disparate cognate and allogeneic pHLA by a single TCR can involve similar binding modes, namely operating via molecular mimicry (Archbold et al., 2008b; Rossjohn and McCluskey, 2007). Here we show that molecular mimicry can underpin human T cell alloreactivity.

RESULTS

Peptide-Dependent Alloreactivity of LC13 T Cells

To investigate the molecular basis of natural human T cell alloreactivity, we examined the prototypic TCR termed LC13 that recognizes the immunodominant HLA-B*0801-restricted epitope, FLRGRAYGL from EBNA 3A of Epstein-Barr virus (EBV) (Argaet et al., 1994; Burrows et al., 1994). LC13 also alloreacts with HLA-B*4402 and HLA-B*4405, related allotypes that differ from each other by only one residue but differ from HLA-B*0801 by 24 and 25 amino acids, respectively.

Alloreactivity can be either dependent or independent of the HLA-bound peptide (Heath et al., 1989, 1991; Smith et al., 1997a, 1997b). Therefore, we examined whether LC13 allorecognition of HLA-B*4405 required a specific peptide(s). Presentation of the HLA-B*4405 alloantigen was examined in transfectants of the class-I-HLA-deficient mutant lymphoblastoid cell line (LCL) C1R and the TAP-deficient T2 cell line (Alexander et al., 1989). The C1R.B*4405 cells, but not the parental C1R cells, were lysed by LC13 cytotoxic T-lymphocyte (CTL), indicating constitutive presentation of an allogeneic ligand by these cells (Figure 1A). However, coexpression of the viral TAP inhibitor ICP47 essentially abolished allorecognition of C1R-B*4405 by LC13 (Figure 1A), indicating TAP dependence of this allogeneic ligand. Exogenous loading of C1R-B*4405-ICP47 cells with viral peptide restored recognition by an antiviral CTL clone (DM1) (Archbold et al., 2009) but did not restore killing by LC13 CTL (Figures 1A and 1B). The T2.B*4405 cell line was not recognized by the human T cell line Jurkat coexpressing the LC13 $\alpha\beta$ TCR and human CD8$\alpha\beta$ genes (LC13.Jurkat) (Beddoe et al., 2009). Stabilization of ''empty'' HLA-B*4405 molecules with a HLA-B*4405-binding peptide (DPα-peptide) did not sensitize the T2.B*4405 cells for recognition by LC13.Jurkat (Figure 1C). Notably, the T2.B*0801 and C1R.B*0801 cell lines loaded with exogenous FLRGRAYGL viral peptide (''virotope'') activated LC13.Jurkat (Figures 1C and 1D), as did C1R.B*4402 and C1R.B*4405 transfectants (Figure 1D). Collectively, these data indicate that the alloreactivity of the LC13 TCR behaved in a peptide-dependent manner.

Identification of a Candidate Allopeptide Presented by HLA-B*4405

A major hurdle in understanding the basis of alloreactivity is the identification of authentic antigenic peptides (the allopeptide[s]) bound to the allogeneic HLA molecule. Murine examples of alloreactive T cells have been the most informative to date, including the alloreactive BM3.3 TCR (Reiser et al., 2000) and the 2C TCR (Colf et al., 2007; Speir et al., 1998) for which pMHC allopeptide structures are solved. However, pathogen-derived cognate ligands for the BM3.3 and 2C T cells remain unknown.

To identify a candidate LC13 allopeptide(s), we generated insect cells expressing individual baculoviral constructs from a library of HLA-B*4405 molecules covalently complexed with randomized peptides. Infected insect cells were screened for interaction with recombinant, bivalent LC13 TCR (Crawford et al., 2006). Repeated rounds of sorting allowed expansion of HLA-B*4405-positive cells expressing a ligand that bound LC13 TCR (Figure 2A). Peptide insert sequences were obtained from 36 positive clones with 30 of these encoding the peptide EEYLKAWTF. Searching the human proteome for analogs of the EEYLKAWTF ''mimotope'' peptide identified two high-scoring matches (expect values of 283 and 65, respectively), each of 9 residues (EESLKDWYF and EEYLQAFTY) and therefore representing a potential natural ''allotope.'' These peptides shared 66% (6/9 identical residues) with the mimotope and possessed the P2E, P9Y/F anchor residues, features of B44-binding peptides. The peptide EESLKDWYF is derived from an ATPase but little is known about its physiologic role and expression. The peptide EEYLQAFTY is derived from an ATP binding cassette protein ABCD3 involved in transport of fatty acids into the peroxisome.

The ABCD3 Allotope Is an Authentic Alloantigen Recognized by LC13

We next examined recognition of the EESLKDWYF or EEYLQAFTY peptides by LC13.Jurkat cells ($CD8^+$) and LC13 CTL. The EESLKDWYF peptide did not activate LC13.Jurkat cells and was not examined further because we conclude that this is not a bona fide alloligand for LC13 (not shown). In contrast, both the mimotope and EEYLQAFTY (hereafter allotope) peptides specifically sensitized exogenously loaded T2-B*4405 cells (Figure 2B, middle) and C1R-B*4405 cells expressing ICP47 (Figure 2B, right) for lysis by LC13 CTL.

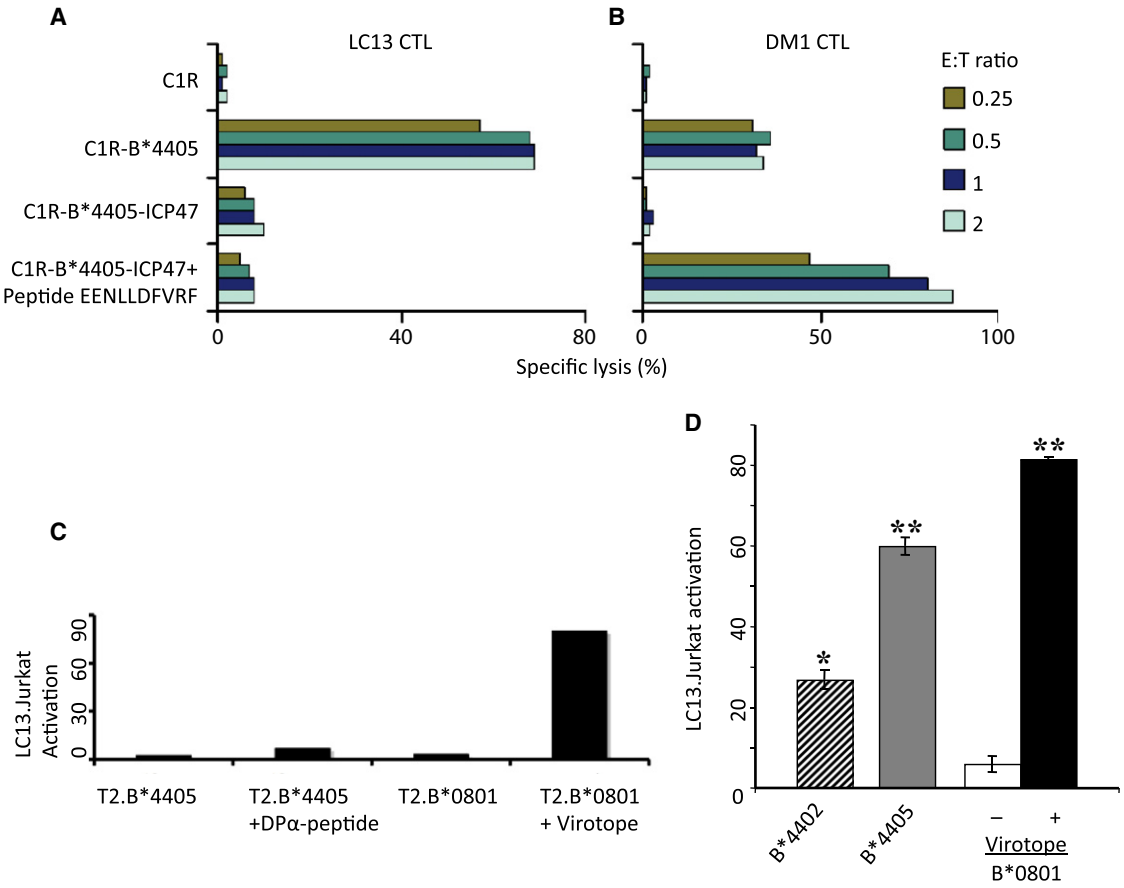

Figure 1. Allorecognition of HLA-B*4405 Is Peptide Dependent

(A and B) The LC13 CTL clone (A) and the HLA-B*4405-restricted CTL clone DM1 (B), specific for the EBV peptide EENLLDFVRF, were tested for killing of the class-I-HLA-negative mutant cell line C1R and its stably transfected derivatives expressing HLA-B*4405 in the presence and absence of the TAP-inhibitor ICP47. Cytotoxicity at four effector:target ratios is shown.

(C) Activation of LC13.Jurkat cells by the TAP-deficient, T2 cell line expressing low levels of HLA-B*4405 (T2.B*4405) and T2 cells expressing HLA-B*0801 (T2.B*0801). T cell activation is shown on the *y* axis as the percentage of CD69-positive cells among the GFP-positive cells.

(D) Activation of LC13.Jurkat cells by the TAP-competent C1R.B*4402 (B*4402), C1R.B*4405 (B*4405), and C1R.B*0801 cell lines as above. C1R.B*0801 transfectants are transformed with a strain of EBV containing a mutation in FLRGRAYGL.

To determine whether the allotope is naturally presented, the impact of super transfection and knockdown of the ABCD3 gene was studied in cells naturally presenting B*4405-restricted alloantigen to LC13. Super transfection of the ABCD3 gene into C1R.B*4405 cells resulted in a modest increase in constitutive activation of LC13.Jurkat by C1R.B*4405 and C1R.B*4402 cells (Figure S1 available online). A specific RNAi construct was also used to knock down the natural, endogenous expression of ABCD3 in Ag-presenting cells (Figure 2C). Real-time PCR assays of RNA expression showed that the ABCD3 allotope RNAi reduced mRNA expression by >80% and confirmed the specificity of the RNAi constructs (semiquantitative RT-PCR inset, Figure 2C and Figure S2). Mock treatment of cells with irrelevant mβ-actin RNAi had no impact on LC13 allorecognition (Figure 2C, middle panel histograms). In contrast, introduction of the ABCD3 RNAi into the C1R.B*4405 cells specifically reduced constitutive activation of LC13.Jurkat T cells by nearly 50% ($p < 0.01$) (Figure 2C, right panel histograms). Addition of exogenous allotope to the knocked down Ag-presenting cells restored full activation of the LC13.Jurkat T cells (Figure 2C). These data indicate that the ABCD3 allotope is an authentic, natural alloantigen recognized by the LC13 TCR.

Molecular Mimicry Underpins LC13 Alloreactivity

To understand the structural basis of the LC13 TCR alloreactivity, we determined the structures of the LC13 TCR in complex with the HLA-B*4405 allotope and mimotope complexes to 2.6 Å and 2.7 Å resolution, respectively (Table 1, Tables S1 and S2). These structures were compared with the LC13-virotope complex (Kjer-Nielsen et al., 2003).

The structure of the LC13 TCR-allotope complex was very similar to the mimotope complex with a root mean square deviation (rmsd) of 0.27 Å over the entire complex, and remarkably, both complexes (Figures 3A and 3B) were very similar to that of the LC13 TCR-virotope complex (Figure 3C; Kjer-Nielsen et al., 2003) (rmsd between the allotope and mimotope complex versus the virotope complex was 0.87 Å and 0.77 Å, respectively). This

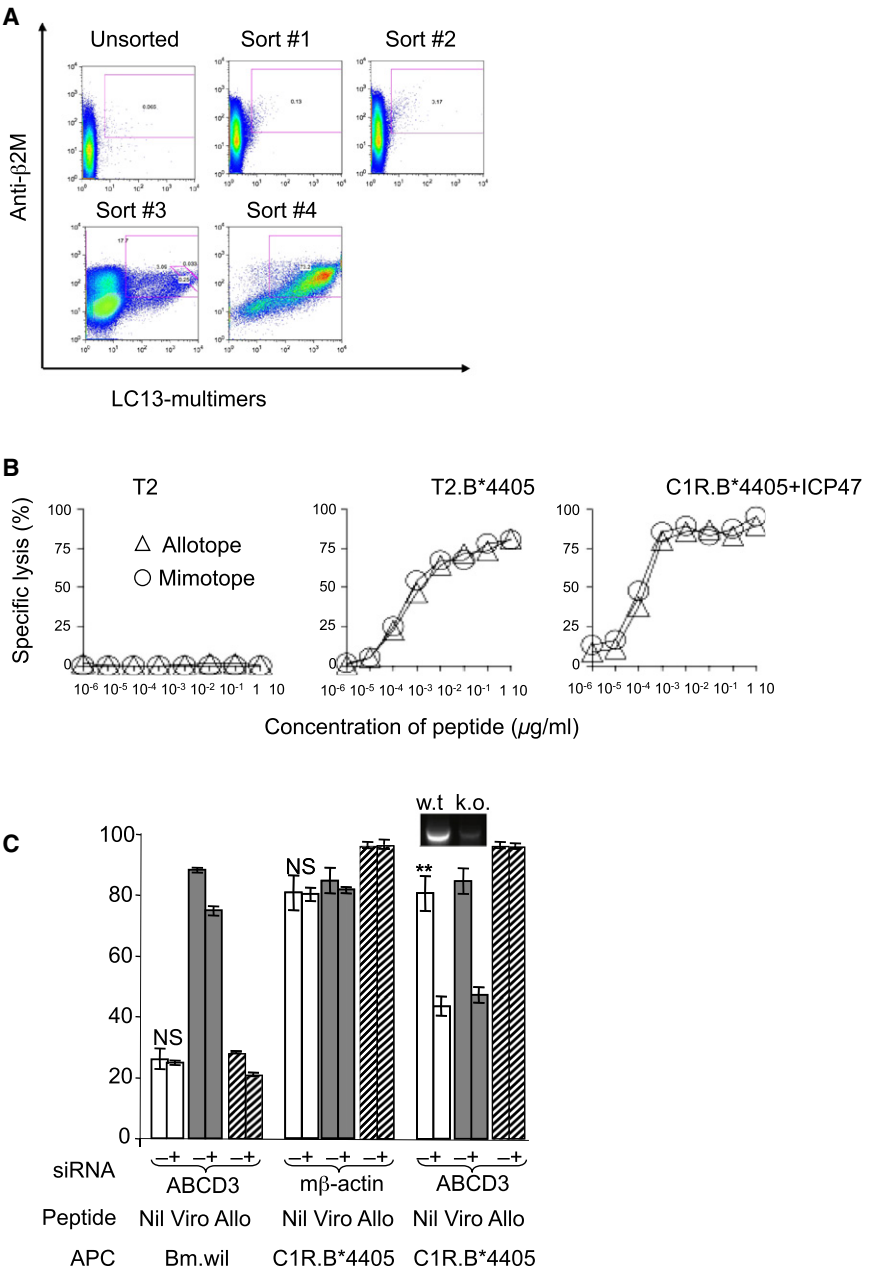

Figure 2. Identification of an Authentic Alloligand Recognized by LC13

(A) Baculovirus-infected insect SF9 cells, each expressing a unique peptide-B*4405 complex on their surface, were costained with anti-β2Microglobulin mAb (*y* axis) and multimeric recombinant LC13 TCR (*x* axis). LC13 staining-SF9 cells were iteratively expanded and sorted. Sequencing of viral constructs consistently identified a single mimotope ligand, EEYLKAWTF.

(B) LC13 recognizes exogenous mimotope and allotope peptides presented by TAP-deficient cells. Dose-dependent recognition of exogenous allotope (triangles) or mimotope (circles) peptide. Cytotoxicity is reported as percent specific lysis by LC13 CTL.

(C) Knockdown of C1R.B4405 recognition by LC13 after RNA interference of ABCD3. The homozygous HLA-B*0801 LCL, Bm.wil, and C1R.B*4405 cell lines were treated with (+) and without (–) ABCD3 or mouse β-actin RNAi constructs and constitutive presentation of alloantigen was assayed in the absence (open bars) or presence of the virotope peptide (Viro) or allotope peptide (Allo). (NS, nonsignificant; **$p < 0.01$). Inset shows an electrophoresis gel photo of PCR amplification of ABCD3 cDNA from C1R.B4405 cells in the presence (KO) and absence (WT) of specific ABCD3 RNAi treatment.

similarity is reflected in the close superposition of the LC13 TCR in these complexes and their identical 60° docking modes across the long axis of the HLA (Figure 3D). Accordingly, the LC13 TCR location over the C terminus of the HLA-B*4405 antigen-binding cleft mimicked the C-terminal docking of the LC13 TCR on the HLA-B*0801-virotope complex (Kjer-Nielsen et al., 2002a, 2003). The total buried surface area (BSA) at the allotope, mimotope, and virotope complexes were all ≈2300 Å^2 and moreover, the shape complementarity at the virotope, allotope, and mimotope interfaces with LC13 was very similar (0.59, 0.64, and 0.60, respectively).

Both the Vα and Vβ domains of the LC13 TCR contributed roughly equally to the interfaces of the allotope, mimotope, and virotope complexes (range: Vα, 51.4%–56.2%, Vβ, 43.8%–48.6%), indicating that the LC13 alloreactivity is not driven by a skewed usage of the V domains at the TCR-pMHC interface unlike other alloreactive complexes (Colf et al., 2007; Reiser et al., 2000). Indeed, the number and nature of the LC13 TCR interactions with the pHLA B*4405 in the allotope and mimotope complexes were also very similar to those of the LC13 TCR-virotope complex (allotope-mimotope-virotope: 146-160-135 van der Waals [v.d.w.] interactions, 15-13-14 H bonds, and 1 salt bridge each; Table S2). Accordingly, the LC13 TCR adopted a strikingly similar footprint on the allogeneic HLA-B*4405-allotope, HLA-B*4405-mimotope, and cognate HLA-B*0801-virotope complex.

Mimicry of the TCR Footprints and Specific Interactions

Although the overall docking modes between the LC13 TCR-allotope, mimotope, and virotope complexes were very similar, this does not confirm molecular mimicry at the molecular level. Therefore, we analyzed the individual contacts of the LC13 TCR with each of these three complexes. The relative contact footprints of the complementarity determining region (CDR) loops at the LC13 TCR-pHLA interfaces were also very similar (Figure 3, bottom). Hence, to varying extents, all the CDR loops of the LC13 TCR contributed to virotope, allotope, and mimotope interactions, with only modest differences between them

Table 1. Data Collection and Refinement Statistics

Data Collection Statistics	LC13-HLA B4405allo	LC13-HLA B4405mimo
Temperature	100K	100K
Space group	***C2***	***C2***
Cell dimensions (a,b,c) (Å, °)	142.52, 54.24, 121.77; β = 114.43	223.12, 53.22, 143.20; β = 102.39
Resolution (Å)	50-2.70 (2.80-2.70)[a]	50-2.60 (2.69-2.60)
Total number of observations	70,144	159,863
Number of unique observations	21,530 (1,278)	50,197 (4,976)
Multiplicity	3.2 (2.0)	3.2 (3.0)
Data completeness (%)	92.0 (55.6)	97.8 (97.8)
I/σ_I	20.1 (2.4)	12.5 (2.3)
R_{merge}[b] (%)	5.9 (25.6)	8.5 (41.1)
Refinement Statistics		
Nonhydrogen atoms		
Protein	6,657	13,316
Water	27	124
Resolution (Å)	2.70	2.60
R_{factor}[c] (%)	19.7	22.1
R_{free}[c] (%)	26.9	27.8
Rms deviations from ideality		
Bond lengths (Å)	0.009	0.006
Bond angles (°)	1.202	0.926
Ramachandran plot (%)		
Most favored region	87.1	90.5
Allowed region	12.0	9.0
Generously allowed region	0.6	0.4

[a] Values in parentheses are for highest-resolution shell.
[b] $R_{merge} = \Sigma \mid I_{hkl} - < I_{hkl} > \mid / \Sigma I_{hkl}$.
[c] $R_{factor} = \Sigma_{hkl} \mid \mid F_o \mid - \mid F_c \mid \mid / \Sigma_{hkl} \mid F_o \mid$ for all data except ≈5% that were used for R_{free} calculation.

(the rmsd of the respective CDR2α, CDR3α, CDR1-3β loops within the complexes was <0.45 Å) (Table S2). One slight difference was the positioning of the CDR1α loop between the allotope and virotope complexes (rmsd approximately 1.0 Å) (not shown). Overall, the conformational changes of the LC13 TCR in forming interactions with the virotope complex (Kjer-Nielsen et al., 2002b, 2003) are mirrored in the interactions with the HLA-B*4405-allotope and mimotope structures, despite the differences in the antigenic peptide sequences.

The CDR1α makes conserved contacts via Gly29α, Thr30α, and Tyr31α with the α2 helix of HLA-B*4405. The Arg62 of HLA-B*4405 contacts the P1 residue of the allotope, and Tyr159 of HLA-B*4405 contacts Thr30α (Figure 4A). Thr30α and Tyr31α enveloped the "gatekeeper" residue Gln155, which changed conformation upon LC13 TCR ligation in all three complexes. Accordingly, the CDR1α loop played a similar role in the overall contribution to interactions in the virotope complex (18.2%) when compared to the allotope and mimotope complexes (16%).

The CDR2α loop of the LC13 TCR contributed equally to the interface in the allotope, mimotope, and virotope interactions (approximately 8%–9%; Figures 3A–3C) and interacted via His48α, Leu50α, Ser52α, and Val55α with the α2 helix of HLA-B*0801 and HLA-B*4405, nestling against the long side chains of Arg151 and Glu154 (Figure 4B). These conserved interactions are mediated predominantly via vdw interactions (Figure 4B; Table S2).

The CDR1β loop minimally participated in the pHLA interactions (Figure 3: Table S2). In contrast, the CDR2β loop contributed equally to the interface in the allotope, virotope, and mimotope interactions (approximately 13%–14%, Figure 4C), through conserved contacts via Tyr48β, Gln50β, Asn51β, Glu52β, and Leu55β and the α1 helix of HLA-B*0801 (residues 72–79) and HLA-B*4405 (residues 72–83). This network of polar-mediated contacts includes one conserved salt bridge between Glu52β and Arg79 (Figure 4C). Ala53β makes an additional contact with Arg75 of HLA-B*4405. Interestingly, the CDR2β loop interacted with HLA-B*4405 position 83, a polymorphic site between HLA-B*4405 (Arg83) and HLA-B*0801 (Gly83) (Figure 4C). However, previous mutagenesis has indicated that the CDR2β loop plays a minor energetic role in the LC13 TCR-HLA-B8-virotope interaction and is therefore unlikely to be important in allogeneic recognition (Borg et al., 2005).

The CDR3α and CDR3β regions contributed approximately equally at the allotope, virotope, and mimotope interfaces (18.9%–21.4% and 24%–25.6%, respectively; Figure 3). The CDR3β loop dominated contacts with the respective peptides (discussed below), whereas the CDR3α loop played a larger role in interacting with the HLA heavy chain α1 helix and also forming interactions with Leu94α and Gln155 of the α2 helix that are conserved across all three complexes (Figure 4D). The conserved interactions between the three complexes also included Gly96α to the aliphatic base of Arg62; Gly97α to Ile66; and contacts via Thr98α and Tyr100α (Figure 4D). Ser99α makes a new B*4405 contact not present in HLA B*0801. The CDR3β loop, which abutted the CDR3α loop and sits centrally above the Ag-binding cleft, mediated contacts with the α1 and the α2 helix of the HLA, in which Gln98β and Tyr100β protruded into the cleft to form conserved interactions along with Leu96β and Gly97β.

Accordingly, a very high degree of mimicry of the cognate HLA-B*0801-virotope underpinned LC13 TCR interactions conserved across the HLA-B*4405-allotope and mimotope complexes.

Peptide-Dependent Molecular Mimicry

Given the differences in the sequences between the cognate virotope, allotope, and mimotope, it was unclear, a priori, whether the peptide-mediated interactions made by the LC13 TCR would be similar between all three complexes. Therefore, we compared the mode of binding of the LC13 TCR to the different peptides.

Upon superposition, the rmsd of the HLA-bound cognate peptide with respect to the bound allotope and mimotope was 0.79 Å and, thus, within the ternary complexes, the peptides adopted similar conformations within the respective Ag-binding cleft (Figure 5). Although the LC13 TCR also interacted with the N-terminal region of the allotope and mimotope peptides (Figures 5A and 5B), the extensive interactions with the

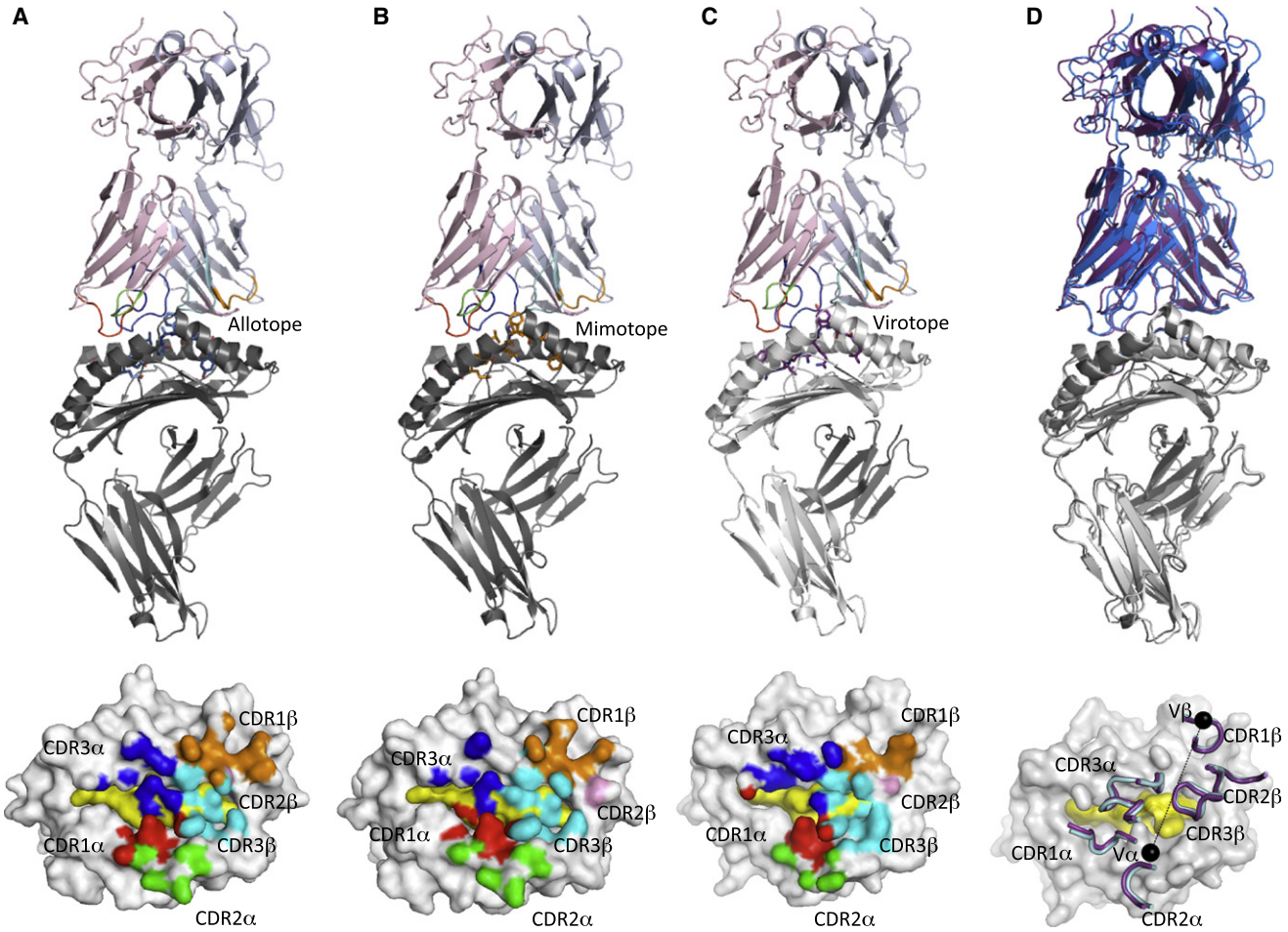

Figure 3. Footprint of LC13 TCR in Complex with HLA-B*4405-Allotope, HLA-B*4405-Mimotope, and HLA-B*0801-Virotope

(A–C) Ribbon representation of the LC13 TCR in complex with HLA-B*4405-allotope (A), HLA-B*4405-mimotope (B), and HLA-B*0801-virotope (C). TCR α chain is in pale pink; the β-chain is in pale blue, HLA-B*4405 is in dark gray, HLA-B*0801 in pale gray, the peptide is in stick format, colored marine for the allotope (A), orange for the mimotope (B), and purple for the virotope (C). Residues contacted by the CDR loops are colored in red (CDR1α), green (CDR2α), blue (CDR3α), orange (CDR1β), pink (CDR2β) and cyan (CDR3β) in the three complexes.

(D) Superposition of LC13 TCR (allotope, blue-green; virotope, purple) in complex with HLA-B*4405-allotope and HLA-B*0801-virotope. The surface representation of HLA-B*0801-virotope at the bottom of the panel shows the CDR loops of the LC13 TCR in complex with HLA-B*4405-allotope (in marine) and with HLA-B*0801-virotope (in purple). The black spheres represent the orientation on the Vα and Vβ chains of the LC13 TCR calculated by center of mass.

C-terminal (P6–8) region of the peptides, known to be critical for recognition of the virotope (Kjer-Nielsen et al., 2003), were highly similar in all three complexes. Namely, the C-terminal residues of both the allotope (P6-Ala, P7-Phe, P8-Thr) and mimotope (P6-Ala, P7-Trp, P8-Thr) include a bulky aromatic side chain at P7 that was flanked by small amino acids, a feature important for LC13 recognition of the virotope (P6-Ala, P7-Tyr, P8-Gly) (Figures 5A–5C; Kjer-Nielsen et al., 2003). Consequently, mimicry in this region underpins how the LC13 TCR interacted with the P6–P8 region of the allotope and the mimotope peptides. The small P6 and P8 residues enabled the P7-aromatic to protrude within a central pocket of the LC13 TCR, as well as contributing to specificity-governing interactions with the LC13 TCR. Namely, the P6-Ala made a conserved interaction with Leu94α of CDR3α and Ala99β of CDR3β, and the backbone of P6-Ala formed a conserved H bond with Gln98β of the CDR3β loop (Figures 5A–5C). Despite the different P8 side chains between the virotope (P8-Gly) and allotope/mimotope (P8-Thr), Tyr100β of the CDR3β loop formed a conserved H bond with the backbone of P8 (Figures 5A–5C). The aromatic structures of the P7 residues were each sandwiched between Tyr31α and Tyr100β and contacted Ala99β (Figures 5A–5C). The P7-Tyr^{OH} of the virotope formed critical water-mediated interactions with His33α and His48α (Figure 5C); however, because of the differences at this position in the mimotope (P7-Trp) and allotope (P7-Phe), these water-mediated interactions were absent in these complexes (Figures 5A and 5B). The P7-Trp of the mimotope formed a H-bond with Tyr31α (Figure 5B). Interestingly, mutating P7-Phe to P7-Tyr of the allotope increased recognition by the LC13 TCR to levels comparable to that of the cognate interaction (data not shown).

These findings also underscore the lack of recognition of the EESLKDWYF candidate peptide identified in the BLASTp search, because the bulky side chain of P8-Tyr in this ligand

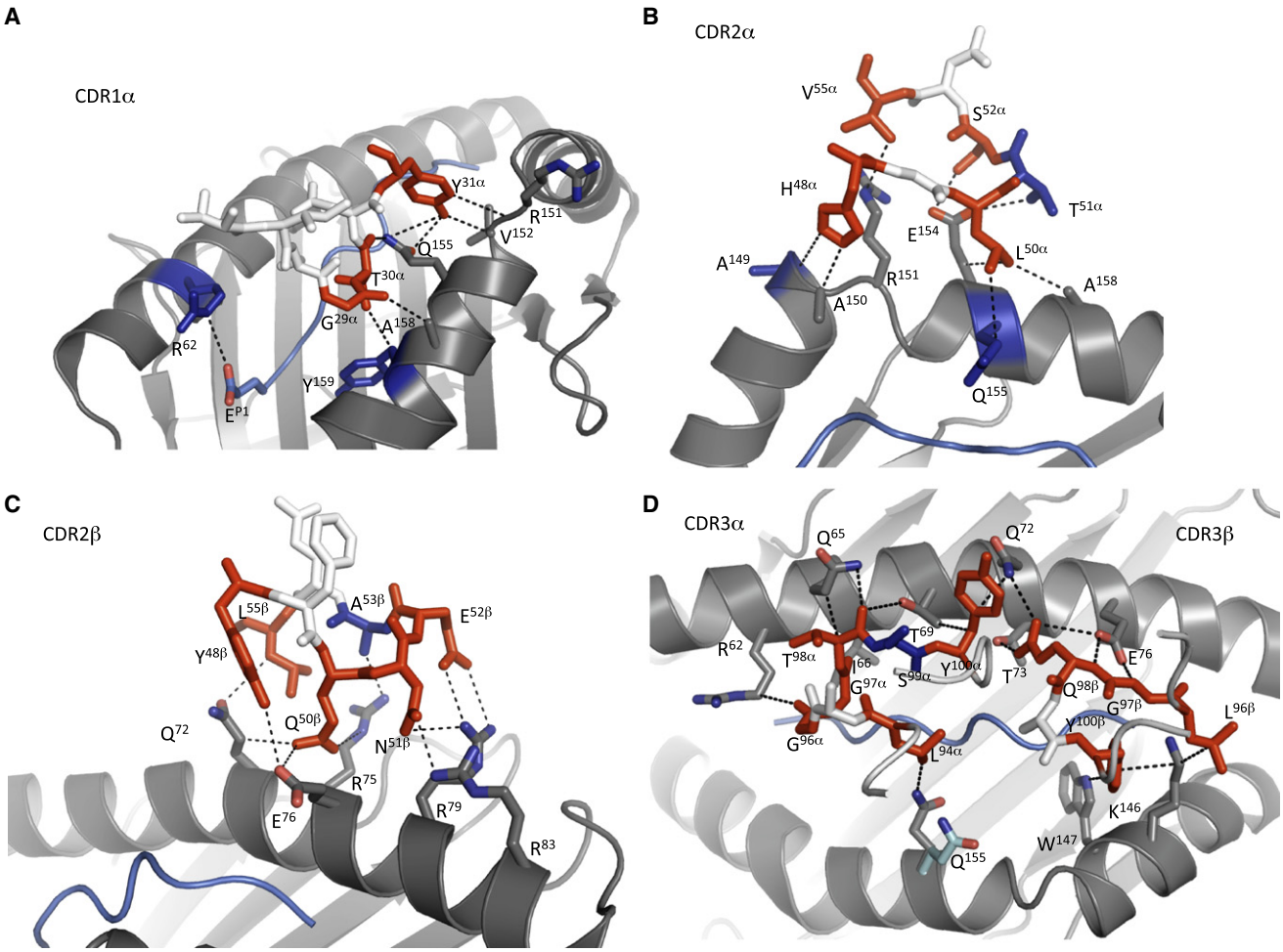

Figure 4. Conserved LC13 TCR Contacts with Cognate and Allogeneic Ligands

Contacts made by the LC13 TCR with the HLA-B*4405-allotope complex. The CDR loops of the LC13 TCR are shown in stick format; the allotope is blue-green and the HLA-B*4405 is dark gray. Interactions between LC13 TCR and HLA-B*4405 that are conserved between LC13 TCR and the HLA-B*0801-virotope are colored in red, and those specific to HLA-B*4405 complex are colored blue. Shown are (A) CDR1α contacts, (B) CDR2α contacts, (C) CDR2β contacts, and (D) CDR3α and CDR3β contacts. Gln155 changes conformation upon ligation and is colored cyan in the nonligated state.

would sterically obstruct recognition of the P7 aromatic crucial to recognition of the B*4405-virotope, allotope, and mimotope complexes. Accordingly, in addition to the mimicry between the surface topology of the HLA-B*0801 and B*4405 heavy chains, substantial mimicry of the HLA-B*0801-restricted virotope underscored how the LC13 TCR interacted with the critical C-terminal region of the HLA-B*4405-restricted allotope and mimotope.

Alloreactivity Discriminates between Related B44 Allotypes

LC13 alloreacts with HLA-B*4402 and HLA-B*4405, but surprisingly not with HLA-B*4403 (Burrows et al., 1994, 1995, 1997). Therefore, we tested LC13 recognition of phytohaemagglutinin (PHA) blast cells expressing either HLA-B*4405, HLA-B*4402, or HLA-B*4403 after adding exogenous mimotope or allotope peptide (Figure 6A). Consistent with the defined specificity of LC13 (Burrows et al., 1997), the HLA-B*4403$^+$ cells were not recognized at physiological concentrations of the mimotope peptide. This might partly reflect lower binding of the allotope peptide to B*4403 (not shown). Interestingly, the HLA-B*4405$^+$ cells presented both peptides more efficiently than did HLA-B*4402. Notably, the allotope and mimotope peptides complexed with HLA-B*4405 were recognized at even lower peptide concentrations than the cognate FLRGRAYGL virotope peptide, presented by HLA-B*0801$^+$ PHA blasts (Figure 6A). This difference appeared to result from differential T cell recognition of these ligands rather than differences in peptide-HLA binding affinity, as shown by the fact that cross-blocking of pHLA-tetramer staining of LC13-like T cells confirmed the binding hierarchy HLA-B*4405-mimotope > HLA-B*4405-allotope > HLA-B*0801-virotope tetramer (Figure S3).

We then tested whether fine specificity of alloreactivity and pHLA-tetramer staining correlated with the affinity of the LC13 TCR-pHLA interaction via surface plasmon resonance (SPR) studies. The LC13 TCR bound to the HLA-B*4405-mimotope complex with comparable affinity to the HLA-B*4402-mimotope complex (Kd = 1.5 μM and 1.3 μM, respectively) but interacted

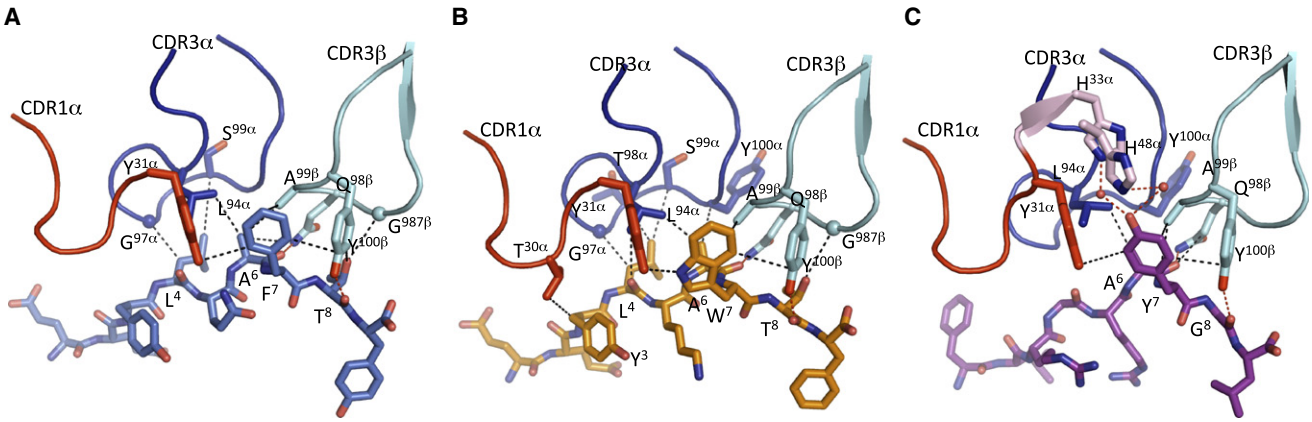

Figure 5. Mimicry in Peptide-TCR Contacts

Contacts between the LC13 TCR and the allotope EEYLQAFTY (dark blue) (A), the mimotope EEYLKAWTF (orange) (B), and the virotope FLRGRAYGL (purple) (C). The peptide is represented in stick format and the LC13 TCR side chains involved in peptide contact are shown. Colors: CDR1α, red; CDR3α, blue; and CDR3β, cyan. The LC13 TCR makes conserved contacts with the allotope (A), mimotope (B), and virotope (C) at positions P6–P8. In addition, the LC13 TCR makes some water-mediated contacts (red dash lines) via His33α and His48α with the Tyr7 of the virotope (C). The interactions made by the LC13 TCR with P4-Leu of both the allotope and mimotope peptides were exclusively via residues from the CDR3α loop and collectively this resulted in a greater contribution of the CDR3α loop in contacting the mimotope (48.5%) and allotope (47%) when compared to the CDR3α-mediated contacts of the virotope (37%). The CDR1α loop of the LC13 TCR contacts P3 of the mimotope.

only very weakly with the HLA-B*4403-mimotope complex (Kd > 200 μM) (Figure 6B; Table S3 and Figure S4). The affinity of the LC13 TCR for the cognate virotope complex fell between these values (Kd ~10–15 μM) (Kjer-Nielsen et al., 2003).

The LC13 TCR bound the HLA-B*4405-allotope complex with a higher affinity than the HLA-B*4402-allotope complex (Kd ~49 μM versus ~189 μM) (Figure 6C; Table S3), whereas binding of the LC13 TCR to the HLA-B*4403-allotope complex was very weak (Kd > 200 μM) (Figure 6C; Figure S4 and Table S3), consistent with the lack of LC13 T cell alloreactivity on HLA-B*4403 (Figure 6A; Burrows et al., 1994, 1995, 1997). Taken together, the cellular recognition and SPR binding studies reflect the intrinsic ability of LC13 TCR to discriminate closely related HLA-B44 allotypes presenting either the mimotope or allotope determinants, despite the hidden nature of the polymorphic HLA residues that distinguish these allotypes.

Molecular Basis for Fine Specificity of Alloreactivity

To better understand how the LC13 TCR could discriminate between HLA-B*4405, HLA-B*4403, and HLA-B*4402 when bound to the allotope and its mimotope, we determined the structures of the six binary pHLA-B44 complexes to high resolution (Table S1 and Figure S5). These three allotypes differ from each other by only 1–2 amino acids in nonexposed positions unable to directly impact on TCR recognition (residue 116 located in the F pocket and/or residue 156 on the α2 helix, D/E pocket). Superposition of the HLA-B*4405, HLA-B*4402, and HLA-B*4403-mimotope complexes revealed virtually no movement of the Ag-binding clefts and modest movements in the peptide attributable to the interactions between the polymorphic residues and the bound peptide (Figure S5). Similarly, superposing the HLA-B*4405, HLA-B*4402, and HLA-B*4403-allotope complexes revealed virtually no movement of the MHC-I heavy chain or the peptide (rmsd 0.18 Å and 0.15 Å, respectively).

The conformation of the allotope and mimotope in their respective LC13-ternary complexes were very similar (rmsd ≈ 0.31 Å) (Figure 6D). However, when the structures of the HLA-B*4405-allotope and HLA-B*4405-mimotope were compared in the absence of LC13 TCR ligation, the conformation of the allotope and the mimotope differed markedly (rmsd 0.94 Å) whereas the HLA Ag-binding cleft adopted the same conformation (rmsd 0.20 Å) (Figure 6E). Namely, there were major differences in the conformation of the peptides between P3-Tyr and P7-Trp/Phe, where, for example, P5-Gln of the allotope and the P5-Lys of the mimotope pointed down or upwards from the Ag-binding cleft, respectively.

This observation revealed that conformational plasticity of the allotope and mimotope play an important role in the alloresponse (compare Figures 6D and 6E). For example, upon ligation, the P3-Tyr of the allotope rotated downwards to avoid steric clashes with Gln155, but nevertheless maintained an H bond with Asp156 and formed an additional H bond to Asp114 (Figure 6F). Additionally, the mimotope is significantly remodeled upon LC13 TCR ligation (Figure 6G). Namely, the CDR1α and CDR3α loops pushed down the central region of the mimotope (Figure 5B), causing P4-Leu to be shifted aside and P5-Lys to flip downwards into the Ag-binding cleft, forming an H bond to Tyr116 and salt bridging to Asp114 and Asp156 (Figure 6G). The movement of Gln155 (Figure 4D) also caused a remodeling of P3-Tyr and P7-Trp, where the P3-Tyr rotated downwards to form a H bond with Asp156 and the P7-Trp side chain flips 180° to establish more contacts with the LC13 TCR. Collectively, the mimotope and allotope mimicked the conformation of the virotope only in the ligated state and thus peptide-dependent molecular mimicry is "forced" by the LC13 TCR (Figures 6D and 6E). However, the LC13 TCR-induced plasticity of the mimotope and allotope would be disfavored in HLA-B*4403 as a result of Leu156. Namely, similar plasticity of the mimotope would result in a buried and uncompensated charge at P5-Lys. Regarding the

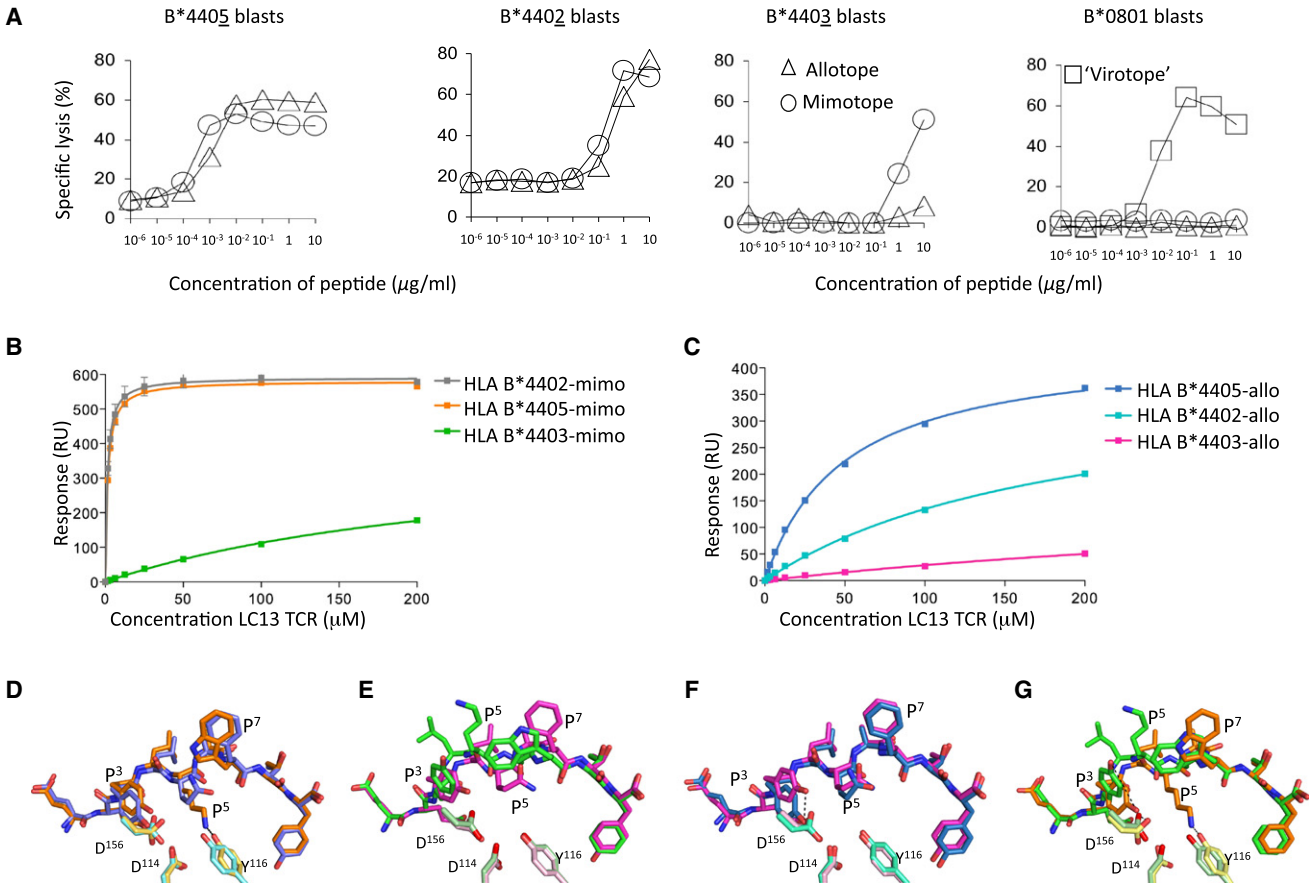

Figure 6. Fine Specificity of the Alloreaction

(A) LC13 recognizes the mimotope and allotope peptides presented by HLA-B*4402 and HLA-B*4405 but not HLA-B*4403. LC13 CTL cytotoxicity of PHA-stimulated T cell lines expressing either HLA-B*4405, HLA-B*4402, or HLA-B*4403. PHA blasts downregulate MHC-I and lose their capacity to be lysed by the LC13 CTLs allowing them to be used as exogenous peptide-presenting targets. Dose response of cytotoxicity on allotope (triangles) or mimotope (circles) peptide. Lysis of HLA-B*0801-positive PHA blasts loaded with the virotope (squares) is also shown.

(B and C) LC13 TCR binding of HLA-B*4405, HLA-B*4402, and HLA-B*4403 in complex with the mimotope (B) and the allotope (C) as determined by SPR.

(D) Superposition of the allotope (blue-green) and the mimotope (orange) bound to the HLA-B*4405 in the LC13 TCR ligated state.

(E) Structure of the allotope (pink) superposed on the mimotope (green) in complex with HLA-B*4405 but unliganded by LC13.

(F) Conformational change of the allotope in the nonligated (pink) and LC13 TCR-ligated state (marine).

(G) Superposition of the mimotope in complex with HLA-B*4405 both unliganded (green) and liganded (orange) to the LC13 TCR. During the LC13 TCR ligation, the mimotope undergoes a structural change with the flipping of Lys5. The polymorphic HLA positions (Tyr116 and Asp156 in HLA-B*4405) and the conserved Asp114 are shown in stick format.

HLA-B*4403-allotope complex, movement of P3-Tyr would result in its hydroxyl moiety being unfavorably located in a hydrophobic pocket. Thus, the fine specificity of the alloreactivity was partly a consequence of the differential ability of HLA-B*4405, HLA-B*4402, and HLA-B*4403 to accommodate plasticity of the mimotope and allotope upon TCR ligation, further highlighting the role and sensitivity of peptide-dependent molecular mimicry.

DISCUSSION

Molecular mimicry, namely when similar structures from dissimilar proteins function in similar ways, is considered to underpin receptor-ligand cross-reactivity in many biological systems (Mariuzza and Poljak, 1993; Oldstone, 1987) and represents a central tenet for therapeutic development of analog drugs. Described in the 1980s in an immunological context (Williams, 1983), molecular mimicry is thought to be the basis for a number of B cell autoimmune disorders, whereby the epitope from the pathogen mimics the conformation of the self-ligand (Oldstone, 1987; Rose and Mackay, 2000). Evidence for molecular mimicry of T cell ligands, though long suspected, has been harder to establish structurally (Quaratino et al., 1995) because of the dual specificity of T cell recognition for MHC and peptide. Nonetheless, evidence is accumulating for mimicry as a basis of some T cell autoimmunity (Harkiolaki et al., 2009; Hausmann et al., 1999; Wucherpfennig and Strominger, 1995) and that T cell cross-reactivity may be dependent on a few conserved germline-encoded interactions (Dai et al., 2008). Here we describe how extensive molecular mimicry underpins direct, human T cell alloreactivity, a structurally unresolved phenomenon that leads to tissue destruction and transplant rejection. In antiviral immunity, small differences in the peptide or HLA molecule can

effectively ablate TCR corecognition of the viral determinant bound to the HLA molecule. Thus, a priori it was unexpected that a human T cell alloreaction between disparate HLA allotypes was attributable to molecular mimicry. Indeed, a previously described example of murine T cell alloreactivity showed how the TCR adopted markedly different docking strategies when recognizing self versus foreign ligands (Colf et al., 2007). To exemplify this point further, HLA-B*4405 differs from HLA-B*0801 by 25 amino acids in the Ag-binding cleft, of which 5 residues (positions 80, 82, 83, 163, and 167) are surface exposed and potentially available for TCR contact. In the 2C TCR system of alloreactivity, H2-K^b and H2-L^d molecules differ by 31 residues, of which only 4 polymorphic residues are solvent exposed for potential TCR contact (Colf et al., 2007). Moreover, if one considers the apparent relatedness between the surface topologies of HLA-B8 and HLA-B44, one would have anticipated that the LC13 TCR alloreacts against all HLA-B44 allotopes, and this is clearly not the case for HLA-B*4403, which differs from HLA-B*4405 by only two buried polymorphic residues (Zernich et al., 2004).

In our study, the viral and allotrope peptides adopted similar conformations only after binding the TCR. This induced-fit mechanism of molecular mimicry further explained why the TCR could effectively discriminate between subtle polymorphic differences between the foreign HLA-B*4402, HLA-B*4405, and HLA-B*4403 allotypes. Thus, our data not only highlight the intricate peptide dependence of T cell alloreactivity but also show that direct T cell alloreactivity is attributable to exquisite specificity of the TCR rather than degenerate recognition of MHC. Our findings suggest that in transplantation, nonpermissive taboo mismatches (Doxiadis et al., 1996) might depend on serendipitous mimicry that is lacking in permissive mismatches.

Our observations in the LC13 TCR system and the contrasting observations in the 2C TCR system raise the intriguing question of whether molecular mimicry, or alternatively, disparate docking modes between the cognate and allo-ligand will best explain the general phenomenon of alloreactivity. The LC13 TCR system describes alloreactivity between two disparate allotypes. Because the LC13 TCR can alloreact via mimicry between these two disparate allotypes, then it follows that alloreactivity between more related alleles is likely to arise from mimicry. Moreover, it also anticipated that molecular mimicry operates between the alloreactions between HLA-B8 and HLA-B*3508 (Archbold et al., 2006) and between HLA-B*3508 and HLA-B44 (Tynan et al., 2005). Moreover, as T cells undergo thymic selection against self-pMHC, they are inherently cross-reactive, and germline-encoded interactions are considered to underpin MHC restriction (Scott-Browne et al., 2009); this further suggests that mimicry will underpin most alloreactions. Consistent with this, recent data (Dai et al., 2008; Rubtsova et al., 2009) suggest that there are conserved CDR1/CDR2 interactions between the cognate pMHC ligands and allogeneic-MHC class II molecules, thereby indicating that molecular mimicry underpins this alloreaction. Nevertheless, more definitive data will be required regarding the relative roles of mimicry versus disparate docking modes typifying alloreactivity, and we suspect that there will be a "sliding scale" between the two examples as suggested by the 2C TCR and LC13 TCR system.

To avoid auto-reactivity, the alloreactive LC13 clonotype is absent from the peripheral T cell repertoire of HLA-B*0801$^+$B*4402$^+$ individuals (Burrows et al., 1995, 1997), instead using an alternative T cell repertoire to recognize the HLA-B8-restricted, FLR-virotope. Similar reshaping of the T cell repertoire occurs in HLA-B*0801$^+$B*4403$^+$ heterozygotes (Burrows et al., 1997), indicating that the LC13 clonotype is sensitive to HLA-B*4403 in the thymus but not in the periphery. This reflects the 30- to 100-fold increased ligand responsiveness of developing T cells compared with mature peripheral T cells (Yagi and Janeway, 1990). Thus, although HLA-B*4403 appears to bind the allotope peptide less efficiently than HLA-B*4405, this determinant is apparently still naturally presented with physiological consequences for the developing T cell repertoire.

In line with molecular mimicry defining the LC13 alloreaction, a prototypical TCR from the virotope-specific T cell repertoire of HLA-B*0801$^+$B*4402$^+$ heterozygous individuals focused on HLA-B*0801 residues that were polymorphic relative to HLA-B44 (Gras et al., 2009). Molecular mimicry and aberrant T cell reactivity represent important and long-standing themes in immunology, and here these concepts converge to provide a basis for understanding peptide-centric T cell alloreactivity.

EXPERIMENTAL PROCEDURES

Cell Lines and Transfectants

The class I reduced human B lymphoblastoid cell line Hmy2.C1R (C1R) expresses HLA-Cw4 and has very low levels of HLA-B*3503 (Zemmour et al., 1992). Transfection of C1R with HLA-B*4402, HLA-B*4403 (Macdonald et al., 2003), or HLA-B*4405 with or without the herpes simplex virus TAP-inhibitor ICP47 has been described previously (Zernich et al., 2004). BM.wil is a human HLA-B*0801 homozygous, lymphoblastoid cell line transformed with Epstein-Barr virus (EBV) (Charron, 1997) and constitutively expressing low levels of EBV antigens including the FLRGRAYGL determinant (Burrows et al., 1994). The T × B hybrid 174 × CEM.T2 (T2) lacks TAP genes and its transfectant derivatives, T2.B*0801 and T2.B*4405, express low levels of "empty" MHC-I gene products at the cell surface (Alexander et al., 1989; Man et al., 1992). Jurkat.LC13 cells were generated by the retroviral transduction of the CD8α and β chains into Jurkat cells, as well as the LC13 TCR α and β genes. The LC13 (Burrows et al., 1994) and DM1 (Archbold et al., 2009) antiviral CTL cones have been previously described.

Identification of Endogenous Alloligand

A randomized peptide library was engineered in complex with HLA-B*4405 molecules in a baculovirus vector (Crawford et al., 2006). The potential nonameric "allopeptide" library was constructed with random oligonucleotides but fixing codons encoding P1E, a residue not likely to be involved in LC13 recognition and the HLA-B*4405 anchor sites P2E and P9F or Y. PCR fragments encoding the library were ligated to constructs encoding β2microglobulin and the HLA-B*4405 heavy chain directing expression of individual HLA-B*4405-peptide complexes from each virus. SF9 cells were infected with the amplified viral stocks containing the HLA-B*4405-peptide library so that each infected cell displayed a unique peptide-HLA complex. Cells were costained with fluoresceinated anti-β2Microglobulin, and fluorochrome-labeled LC13 TCR ectodomain made multimeric with an anti-TCR mAb. Rare cells expressing HLA-B*4405-peptide complexes that bound LC13 TCR were repeatedly sorted and expanded by culture in vitro. After the 4th sorting, SF9 cells homogeneously expressed a ligand that bound both anti-β2Microglobulin and multimeric LC13.

T Cell Activation Assays

CTL killing assays (Burrows et al., 1994) and activation of Jurkat.LC13 cells were assayed as previously described (Beddoe et al., 2009). Essentially, Jurkat.LC13 cells (10^5) were cocultured with 10^5 antigen-presenting cells for 4 hr at 37°C in the absence or presence of peptide. Expression of CD69 was

then detected by flow cytometry gating on GFP-positive LC13.Jurkat cells. T cell activation was measured as the percentage of CD69-positive cells among the GFP-positive LC13.Jurkat cells relative to the unstimulated population. RNAi knockdown of ABCD3 is described in the Supplemental Data. Primary T cells were obtained from blood donors with the approval of the Australian Bone Marrow Donor Registry Ethics Committee Scientific Review Panel.

Additional Data

Supplemental Data include protein expression, purification, crystallization, structure determination, and SPR measurement.

ACCESSION NUMBERS

Coordinates have been deposited in the PDB (codes: 3KPL, 3KPM, 3KPN, 3KPO, 3KPP, 3KPQ, 3KPS, 3KPR).

SUPPLEMENTAL DATA

Supplemental Data include Supplemental Experimental Procedures, seven figures, and three tables and can be found with this article online at http://www.cell.com/immunity/supplemental/S1074-7613(09)00510-X.

ACKNOWLEDGMENTS

We thank the staff at the GMCA-CAT beamline (Chicago, Advanced Photon Source) and the PX1 Beamline at the Australian synchrotron for assistance with data collection. We thank Hugh Reid and Kim R. Jordan for technical advice. J.R. is a Federation Fellow of the Australian Research Council, C.S.C. is an ARC QEII fellow, W.A.M. is a Peter Doherty Postdoctoral Fellow, F.E.T. is a CJ Martin Fellow, and A.W.P., M.C.J.W., and S.R.B. are Senior Research Fellows of the National Health and Medical Research Council Australia. This work was supported by grants from the ARC, NHMRC, and Roche Organ Transplant Research Foundation.

Received: June 10, 2009
Revised: September 10, 2009
Accepted: September 25, 2009
Published online: December 17, 2009

REFERENCES

Afzali, B., Lechler, R.I., and Hernandez-Fuentes, M.P. (2007). Allorecognition and the alloresponse: clinical implications. Tissue Antigens *69*, 545–556.

Alexander, J., Payne, J.A., Murray, R., Frelinger, J.A., and Cresswell, P. (1989). Differential transport requirements of HLA and H-2 class I glycoproteins. Immunogenetics *29*, 380–388.

Archbold, J.K., Macdonald, W.A., Miles, J.J., Brennan, R.M., Kjer-Nielsen, L., McCluskey, J., Burrows, S.R., and Rossjohn, J. (2006). Alloreactivity between disparate cognate and allogeneic pMHC-I complexes is the result of highly focused, peptide-dependent structural mimicry. J. Biol. Chem. *281*, 34324–34332.

Archbold, J.K., Ely, L.K., Kjer-Nielsen, L., Burrows, S.R., Rossjohn, J., McCluskey, J., and Macdonald, W.A. (2008a). T cell allorecognition and MHC restriction—A case of Jekyll and Hyde? Mol. Immunol. *45*, 583–598.

Archbold, J.K., Macdonald, W.A., Burrows, S.R., Rossjohn, J., and McCluskey, J. (2008b). T-cell allorecognition: A case of mistaken identity or déjà vu? Trends Immunol. *29*, 220–226.

Archbold, J.K., Macdonald, W.A., Gras, S., Ely, L.K., Miles, J.J., Bell, M.J., Brennan, R.M., Beddoe, T., Wilce, M.C.J., Clements, C.S., et al. (2009). Natural micropolymorphism in human leukocyte antigens provides a basis for genetic control of antigen recognition. J. Exp. Med. *206*, 209–219.

Argaet, V.P., Schmidt, C.W., Burrows, S.R., Silins, S.L., Kurilla, M.G., Doolan, D.L., Suhrbier, A., Moss, D.J., Kieff, E., Sculley, T.B., and Misko, I.S. (1994). Dominant selection of an invariant T cell antigen receptor in response to persistent infection by Epstein-Barr virus. J. Exp. Med. *180*, 2335–2340.

Beddoe, T., Chen, Z., Clements, C.S., Ely, L.K., Bushell, S.R., Vivian, J.P., Kjer-Nielsen, L., Pang, S.S., Dunstone, M.A., Liu, Y.C., et al. (2009). Antigen ligation triggers a conformational change within the constant domain of the alphabeta T cell receptor. Immunity *30*, 777–788.

Bevan, M.J. (1984). High determinant density may explain the phenomenon of alloreactivity. Immunol. Today *5*, 128–130.

Bevan, M.J., and Hünig, T. (1981). T cells respond preferentially to antigens that are similar to self H-2. Proc. Natl. Acad. Sci. USA *78*, 1843–1847.

Borg, N.A., Ely, L.K., Beddoe, T., Macdonald, W.A., Reid, H.H., Clements, C.S., Purcell, A.W., Kjer-Nielsen, L., Miles, J.J., Burrows, S.R., et al. (2005). The CDR3 regions of an immunodominant T cell receptor dictate the 'energetic landscape' of peptide-MHC recognition. Nat. Immunol. *6*, 171–180.

Borg, N.A., Wun, K.S., Kjer-Nielsen, L., Wilce, M.C., Pellicci, D.G., Koh, R., Besra, G.S., Bharadwaj, M., Godfrey, D.I., McCluskey, J., and Rossjohn, J. (2007). CD1d-lipid-antigen recognition by the semi-invariant NKT T-cell receptor. Nature *448*, 44–49.

Burrows, S.R., Khanna, R., Burrows, J.M., and Moss, D.J. (1994). An alloresponse in humans is dominated by cytotoxic T lymphocytes (CTL) cross-reactive with a single Epstein-Barr virus CTL epitope: implications for graft-versus-host disease. J. Exp. Med. *179*, 1155–1161.

Burrows, S.R., Silins, S.L., Moss, D.J., Khanna, R., Misko, I.S., and Argaet, V.P. (1995). T cell receptor repertoire for a viral epitope in humans is diversified by tolerance to a background major histocompatibility complex antigen. J. Exp. Med. *182*, 1703–1715.

Burrows, S.R., Silins, S.L., Cross, S.M., Peh, C.A., Rischmueller, M., Burrows, J.M., Elliott, S.L., and McCluskey, J. (1997). Human leukocyte antigen phenotype imposes complex constraints on the antigen-specific cytotoxic T lymphocyte repertoire. Eur. J. Immunol. *27*, 178–182.

Charron, D. (1997). Genetic Diversity of HLA Functional and Medical Implication, Volume 1 (Paris: EDK Medical and Scientific International Publisher).

Colf, L.A., Bankovich, A.J., Hanick, N.A., Bowerman, N.A., Jones, L.L., Kranz, D.M., and Garcia, K.C. (2007). How a single T cell receptor recognizes both self and foreign MHC. Cell *129*, 135–146.

Crawford, F., Jordan, K.R., Stadinski, B., Wang, Y., Huseby, E., Marrack, P., Slansky, J.E., and Kappler, J.W. (2006). Use of baculovirus MHC/peptide display libraries to characterize T-cell receptor ligands. Immunol. Rev. *210*, 156–170.

Dai, S., Huseby, E.S., Rubtsova, K., Scott-Browne, J., Crawford, F., Macdonald, W.A., Marrack, P., and Kappler, J.W. (2008). Crossreactive T Cells spotlight the germline rules for alphabeta T cell-receptor interactions with MHC molecules. Immunity *28*, 324–334.

Davis, M.M., Boniface, J.J., Reich, Z., Lyons, D., Hampl, J., Arden, B., and Chien, Y. (1998). Ligand recognition by alpha beta T cell receptors. Annu. Rev. Immunol. *16*, 523–544.

Doxiadis, I.I., Smits, J.M., Schreuder, G.M., Persijn, G.G., van Houwelingen, H.C., van Rood, J.J., and Claas, F.H. (1996). Association between specific HLA combinations and probability of kidney allograft loss: The taboo concept. Lancet *348*, 850–853.

Dröge, W. (1979). Hypothesis on the origin of the strong alloreactivity. Immunobiology *156*, 2–12.

Felix, N.J., Donermeyer, D.L., Horvath, S., Walters, J.J., Gross, M.L., Suri, A., and Allen, P.M. (2007). Alloreactive T cells respond specifically to multiple distinct peptide-MHC complexes. Nat. Immunol. *8*, 388–397.

Fink, P.J., and Bevan, M.J. (1995). Positive selection of thymocytes. Adv. Immunol. *59*, 99–133.

Fleischhauer, K., Kernan, N.A., O'Reilly, R.J., Dupont, B., and Yang, S.Y. (1990). Bone marrow-allograft rejection by T lymphocytes recognizing a single amino acid difference in HLA-B44. N. Engl. J. Med. *323*, 1818–1822.

Garboczi, D.N., and Biddison, W.E. (1999). Shapes of MHC restriction. Immunity *10*, 1–7.

Garcia, K.C., Degano, M., Pease, L.R., Huang, M., Peterson, P.A., Teyton, L., and Wilson, I.A. (1998). Structural basis of plasticity in T cell receptor recognition of a self peptide-MHC antigen. Science *279*, 1166–1172.

Garcia, K.C., Degano, M., Speir, J.A., and Wilson, I.A. (1999). Emerging principles for T cell receptor recognition of antigen in cellular immunity. Rev. Immunogenet. *1*, 75–90.

Gras, S., Burrows, S.R., Kjer-Nielsen, L., Clements, C.S., Liu, Y.C., Sullivan, L.C., Bell, M.J., Brooks, A.G., Purcell, A.W., McCluskey, J., and Rossjohn, J. (2009). The shaping of T cell receptor recognition by self-tolerance. Immunity *30*, 193–203.

Harkiolaki, M., Holmes, S.L., Svendsen, P., Gregersen, J.W., Jensen, L.T., McMahon, R., Friese, M.A., van Boxel, G., Etzensperger, R., Tzartos, J.S., et al. (2009). T cell-mediated autoimmune disease due to low-affinity cross-reactivity to common microbial peptides. Immunity *30*, 348–357.

Hausmann, S., Martin, M., Gauthier, L., and Wucherpfennig, K.W. (1999). Structural features of autoreactive TCR that determine the degree of degeneracy in peptide recognition. J. Immunol. *162*, 338–344.

Heath, W.R., Hurd, M.E., Carbone, F.R., and Sherman, L.A. (1989). Peptide-dependent recognition of H-2Kb by alloreactive cytotoxic T lymphocytes. Nature *341*, 749–752.

Heath, W.R., Kane, K.P., Mescher, M.F., and Sherman, L.A. (1991). Alloreactive T cells discriminate among a diverse set of endogenous peptides. Proc. Natl. Acad. Sci. USA *88*, 5101–5105.

Heemskerk, M.B., Cornelissen, J.J., Roelen, D.L., van Rood, J.J., Claas, F.H., Doxiadis, I.I., and Oudshoorn, M. (2007). Highly diverged MHC class I mismatches are acceptable for haematopoietic stem cell transplantation. Bone Marrow Transplant. *40*, 193–200.

Hogquist, K.A., Gavin, M.A., and Bevan, M.J. (1993). Positive selection of CD8+ T cells induced by major histocompatibility complex binding peptides in fetal thymic organ culture. J. Exp. Med. *177*, 1469–1473.

Jameson, S.C., Hogquist, K.A., and Bevan, M.J. (1995). Positive selection of thymocytes. Annu. Rev. Immunol. *13*, 93–126.

Kawase, T., Morishima, Y., Matsuo, K., Kashiwase, K., Inoko, H., Saji, H., Kato, S., Juji, T., Kodera, Y., Sasazuki, T., and Japan Marrow Donor Program. (2007). High-risk HLA allele mismatch combinations responsible for severe acute graft-versus-host disease and implication for its molecular mechanism. Blood *110*, 2235–2241.

Keever, C.A., Leong, N., Cunningham, I., Copelan, E.A., Avalos, B.R., Klein, J., Kapoor, N., Adams, P.W., Orosz, C.G., Tutschka, P.J., et al. (1994). HLA-B44-directed cytotoxic T cells associated with acute graft-versus-host disease following unrelated bone marrow transplantation. Bone Marrow Transplant. *14*, 137–145.

Kjer-Nielsen, L., Clements, C.S., Brooks, A.G., Purcell, A.W., Fontes, M.R., McCluskey, J., and Rossjohn, J. (2002a). The structure of HLA-B8 complexed to an immunodominant viral determinant: peptide-induced conformational changes and a mode of MHC class I dimerization. J. Immunol. *169*, 5153–5160.

Kjer-Nielsen, L., Clements, C.S., Brooks, A.G., Purcell, A.W., McCluskey, J., and Rossjohn, J. (2002b). The 1.5 A crystal structure of a highly selected antiviral T cell receptor provides evidence for a structural basis of immunodominance. Structure *10*, 1521–1532.

Kjer-Nielsen, L., Clements, C.S., Purcell, A.W., Brooks, A.G., Whisstock, J.C., Burrows, S.R., McCluskey, J., and Rossjohn, J. (2003). A structural basis for the selection of dominant alphabeta T cell receptors in antiviral immunity. Immunity *18*, 53–64.

Lechler, R., and Lombardi, G. (1990). The structural basis of alloreactivity. Immunol. Res. *9*, 135–146.

Lindahl, K.F., and Wilson, D.B. (1977). Histocompatibility antigen-activated cytotoxic T lymphocytes. I. Estimates of the absolute frequency of killer cells generated in vitro. J. Exp. Med. *145*, 500–507.

Macdonald, W.A., Purcell, A.W., Mifsud, N.A., Ely, L.K., Williams, D.S., Chang, L., Gorman, J.J., Clements, C.S., Kjer-Nielsen, L., Koelle, D.M., et al. (2003). A naturally selected dimorphism within the HLA-B44 supertype alters class I structure, peptide repertoire, and T cell recognition. J. Exp. Med. *198*, 679–691.

Man, S., Salter, R.D., and Engelhard, V.H. (1992). Role of endogenous peptide in human alloreactive cytotoxic T cell responses. Int. Immunol. *4*, 367–375.

Mariuzza, R.A., and Poljak, R.J. (1993). The basics of binding: Mechanisms of antigen recognition and mimicry by antibodies. Curr. Opin. Immunol. *5*, 50–55.

Matzinger, P., and Bevan, M.J. (1977). Hypothesis: Why do so many lymphocytes respond to major histocompatibility antigens? Cell. Immunol. *29*, 1–5.

Mifsud, N.A., Purcell, A.W., Chen, W., Holdsworth, R., Tait, B.D., and McCluskey, J. (2008). Immunodominance hierarchies and gender bias in direct T(CD8)-cell alloreactivity. Am. J. Transplant. *8*, 121–132.

Oldstone, M.B. (1987). Molecular mimicry and autoimmune disease. Cell *50*, 819–820.

Parham, P., and Ohta, T. (1996). Population biology of antigen presentation by MHC class I molecules. Science *272*, 67–74.

Quaratino, S., Thorpe, C.J., Travers, P.J., and Londei, M. (1995). Similar antigenic surfaces, rather than sequence homology, dictate T-cell epitope molecular mimicry. Proc. Natl. Acad. Sci. USA *92*, 10398–10402.

Reiser, J.B., Darnault, C., Guimezanes, A., Grégoire, C., Mosser, T., Schmitt-Verhulst, A.M., Fontecilla-Camps, J.C., Malissen, B., Housset, D., and Mazza, G. (2000). Crystal structure of a T cell receptor bound to an allogeneic MHC molecule. Nat. Immunol. *1*, 291–297.

Rose, N.R., and Mackay, I.R. (2000). Molecular mimicry: a critical look at exemplary instances in human diseases. Cell. Mol. Life Sci. *57*, 542–551.

Rossjohn, J., and McCluskey, J. (2007). How a home-grown T cell receptor interacts with a foreign landscape. Cell *129*, 19–20.

Rubtsova, K., Scott-Browne, J.P., Crawford, F., Dai, S., Marrack, P., and Kappler, J.W. (2009). Many different Vbeta CDR3s can reveal the inherent MHC reactivity of germline-encoded TCR V regions. Proc. Natl. Acad. Sci. USA *106*, 7951–7956.

Rudolph, M.G., Stanfield, R.L., and Wilson, I.A. (2006). How TCRs bind MHCs, peptides, and coreceptors. Annu. Rev. Immunol. *24*, 419–466.

Scott-Browne, J.P., White, J., Kappler, J.W., Gapin, L., and Marrack, P. (2009). Germline-encoded amino acids in the alphabeta T-cell receptor control thymic selection. Nature *458*, 1043–1046.

Sherman, L.A., and Chattopadhyay, S. (1993). The molecular basis of allorecognition. Annu. Rev. Immunol. *11*, 385–402.

Smith, K.D., Huczko, E., Engelhard, V.H., Li, Y.Y., and Lutz, C.T. (1997a). Alloreactive cytotoxic T lymphocytes focus on specific major histocompatibility complex-bound peptides. Transplantation *64*, 351–359.

Smith, P.A., Brunmark, A., Jackson, M.R., and Potter, T.A. (1997b). Peptide-independent recognition by alloreactive cytotoxic T lymphocytes (CTL). J. Exp. Med. *185*, 1023–1033.

Speir, J.A., Garcia, K.C., Brunmark, A., Degano, M., Peterson, P.A., Teyton, L., and Wilson, I.A. (1998). Structural basis of 2C TCR allorecognition of H-2Ld peptide complexes. Immunity *8*, 553–562.

Tynan, F.E., Burrows, S.R., Buckle, A.M., Clements, C.S., Borg, N.A., Miles, J.J., Beddoe, T., Whisstock, J.C., Wilce, M.C., Silins, S.L., et al. (2005). T cell receptor recognition of a 'super-bulged' major histocompatibility complex class I-bound peptide. Nat. Immunol. *6*, 1114–1122.

Williams, R.C., Jr. (1983). Rheumatic fever and the streptococcus. Another look at molecular mimicry. Am. J. Med. *75*, 727–730.

Wucherpfennig, K.W., and Strominger, J.L. (1995). Molecular mimicry in T cell-mediated autoimmunity: viral peptides activate human T cell clones specific for myelin basic protein. Cell *80*, 695–705.

Yagi, J., and Janeway, C.A., Jr. (1990). Ligand thresholds at different stages of T cell development. Int. Immunol. *2*, 83–89.

Zemmour, J., Little, A.M., Schendel, D.J., and Parham, P. (1992). The HLA-A,B "negative" mutant cell line C1R expresses a novel HLA-B35 allele, which also has a point mutation in the translation initiation codon. J. Immunol. *148*, 1941–1948.

Zernich, D., Purcell, A.W., Macdonald, W.A., Kjer-Nielsen, L., Ely, L.K., Laham, N., Crockford, T., Mifsud, N.A., Bharadwaj, M., Chang, L., et al. (2004). Natural HLA class I polymorphism controls the pathway of antigen presentation and susceptibility to viral evasion. J. Exp. Med. *200*, 13–24.

Zinkernagel, R.M., and Doherty, P.C. (1974). Restriction of in vitro T cell-mediated cytotoxicity in lymphocytic choriomeningitis within a syngeneic or semi-allogeneic system. Nature *248*, 701–702.